Electron Density Analysis on the Protonation of Nitriles

José Luis López, Ana M. Graña, and Ricardo A. Mosquera*

Departamento Química Física, Universidade de Vigo, Lagoas-Marcosende, 36310-Vigo, Galicia (Spain)

Received: December 14, 2008; Revised Manuscript Received: January 9, 2009

The applicability of the resonance model to explain the evolution of electron density was tested for a set of 15 nitriles whose protonation processes were studied by means of the quantum theory of atoms in molecules (QTAIM). The electron densities were obtained at the B3LYP/6-31++G**//B3LYP/6-31++G** and HF/6-31++G**//HF/6-31++G** levels. QTAIM atomic and bond properties do not follow the trends that should be expected according to the resonance model and our results are more in line with a $H^+-N{\equiv}C-R$ Lewis structure than with the $H-N^+{\equiv}C-R$ and $H-N{=}C^+-R$ ones. Also, reasonable agreement between experimental and calculated PA values as well as good correlations between variations in atomic energies and populations as a result of protonation were found.

Introduction

The applicability of the resonance model (RM) to explain the structure and reactivity of organic compounds has been generally accepted[1,2] and has proved to be a very useful tool in chemistry. Nevertheless, topological analysis of electron densities carried out with the quantum theory atoms in molecules (QTAIM)[3,4] for diverse processes have reported evolutions of the electron density that are not in line with the predictions provided by the RM. These disagreements appear even for so simple processes as internal rotations,[5,6] protonations,[7−9] or hydride additions.[10] Also, QTAIM results are inconsistent with the Lewis structures traditionally accepted for some charged compounds, like diazonium salts[11] or protonated ethers.[12−14] The publication of the first study reporting on the disagreements between RM and QTAIM was followed by a controversy about the suitability of QTAIM for this kind of studies.[15−17] Nowadays, this controversy seems to be solved clearly in favor of QTAIM applicability.[16,17] Moreover, most of the qualitative conclusions obtained from QTAIM studies on protonation and hydride addition are confirmed by other electron density analysis,[9,10] like Hirshfeld partitioning.[18,19]

$H-N{=}C^+-R$ Lewis structures have been traditionally employed for describing protonated nitriles in diverse reaction mechanisms. These structures are, in the context of the RM, the result of transforming one π electron pair of the N≡C triple bond into the N−H bond. Alternatively, the protonation process could be understood as the formation of a dative bond between N and proton using the nitrogen lone pair, a process represented by the $H-N^+{\equiv}C-R$ resonance form. These are basically the same schemes used for explaining protonations at other electronegative sites, which have been recently found in controversy with the QTAIM studies carried out for the N-protonation of indole,[20] O-protonation of simple carbonyl systems,[9] and N/O-protonations on diverse pyrimidinic bases.[7,8,21] All of these studies point to H^+-X-R structures (X=O or N and the X−R bond being single or double). QTAIM results for these systems also indicate that the formation of the H^+-X bond is accompanied by an electron density redistribution affecting the whole molecule. Hydrogens act very effectively as a source of electron density for this redistribution, as reported by Stuchbury and Cooper studying the basicity of NH_3 and the series of methylamines.[22]

In this work, we have carried out a QTAIM study on the protonation of several cyanocompounds. This allows to study if the triple bonding modifies the trends hitherto observed for other compounds. The molecules here studied include both linear and branched cyanoalkanes as well as compounds where the cyano function is conjugated with π delocalized systems. Thus, we have been able to establish trends for the size of linear alkyl chains (**1**−**6**), conformational change (**4**, **7**), alkyl chain ramification (**2**, **3**, **8**, **9**), electronegativity of the substitutents (**2**, **10**), and π-delocalization (**11**−**15**) (Table 1).

Computational Details

QTAIM allows the partitioning of a molecule into disjoint subsystems without resorting to hypothesis alien to quantum mechanics.[3,4] With a few exceptions,[23] each of these subsystems consists of a nucleus, which acts as an attractor for the trajectories of the gradient of the electron density vector field, $\nabla\rho(\mathbf{r})$, and its associated atomic basin, throughout these trajectories spread. An atom, Ω, is defined as the union of the attractor and its associated basin, and it is surrounded by zero flux surfaces for $\nabla\rho(\mathbf{r})$. The integration of the proper density functions within these limits provides diverse atomic properties such as the electron population, $N(\Omega)$, or the total atomic electron energy, $E(\Omega)$. In this article, we have considered the σ and π components of the atomic electron population, $N^{\sigma}(\Omega)$ and $N^{\pi}(\Omega)$, respectively.

QTAIM also recovers main elements of molecular structure in terms of the critical points, $\mathbf{r}_c$, of the electron density, $\rho(\mathbf{r})$. Prominent among them are the bond critical points (BCPs), which are located roughly in between every pair of bonded atoms. Although the relationship between the presence of a BCP and the existence of a chemical bonding has become a controversial and it is still a debated point of the theory,[24−29] the electron density at a certain BCP is regarded as an indicator for bond strength.

All the neutral (**1** to **15**) and protonated (**1**+ to **15**+) species here considered (Table 1) were fully optimized at the HF/6-31++G(d,p) and B3LYP/6-31++G(d,p) levels using the program *GAMESS*.[32] The optimization was performed using the self-consistent virial scaling (SCVS) method introduced by Lehd

* To whom correspondence should be addressed.

10.1021/jp811023x CCC: $40.75
Published on Web 02/23/2009

TABLE 1: Proton Affinities (kJ mol^{-1}) and Accuracy Estimators for QTAIM Integrations for the R−C≡N Molecules Here Studied

	R	PA (HF)	PA (B3LYP)	PA[a]	$N - \Sigma N(\Omega)$[b]	$E - \Sigma E(\Omega)$[c]	$\lvert L(\Omega)\rvert$[d]
1	H	721.1	710.3	712.9	−0.4 (0.0)[f]	−0.4 (−0.2)[f]	0.5
2	CH_3	791.7	786.4	779.2	0.1 (0.0)	0.1 (−0.2)	0.2
3	CH_3CH_2	804.7	800.2	794.1	−0.6 (0.2)	−0.4 (0.0)	0.1
4	$CH_3(CH_2)_2$ anti	810.7	807.3	798.4[e]	0.2 (0.4)	0.1 (0.1)	0.9
5	$CH_3(CH_2)_3$	811.5	810.8	802.4	1.2 (1.9)	0.7 (1.2)	0.7
6	$CH_3(CH_2)_4$	813.5	814.1		−0.3 (1.2)	−0.2 (0.7)	0.8
7	$CH_3(CH_2)_2$ gauche	810.2	807.0		−1.5 (−0.3)	−0.9 (−0.4)	0.1
8	$CH(CH_3)_2$	815.1	810.6	803.6	−0.1 (0.4)	−0.2 (0.0)	0.7
9	$C(CH_3)_3$	824.1	820.6	810.9	1.0 (0.2)	0.5 (−0.2)	0.9
10	CF_3	678.8	671.8	688.4	0.3 (0.7)	0.0 (0.2)	0.5
11	CH_2=CH	802.7	795.2	784.7	−0.6 (0.2)	−0.8 (0.5)	1.0
12	CH_2=CH−CH=CH	836.7	835.6		1.0 (−0.6)	−1.0 (−0.6)	0.9
13	C_6H_5	826.6	829.4	811.5	2.0 (0.8)	1.0 (0.1)	0.9
14	$C_{10}H_7$ (α)	849.0	848.3		−0.6 (0.1)	−0.5 (0.2)	0.4
15	$C_{10}H_7$ (β)	849.4	848.8		−0.1 (0.4)	−0.6 (0.7)	1.3

[a] Experimental values taken from ref 37. [b] Values in au multiplied by 10^3. [c] In kJ mol^{-1}. [d] Maximum absolute value of integrated $L(\Omega)$ in the neutral molecule and its protonated species, in au multiplied by 10^3. [e] Experimental value assigned to the most stable conformer in this table. [f] Values for protonated species in parenthesis.

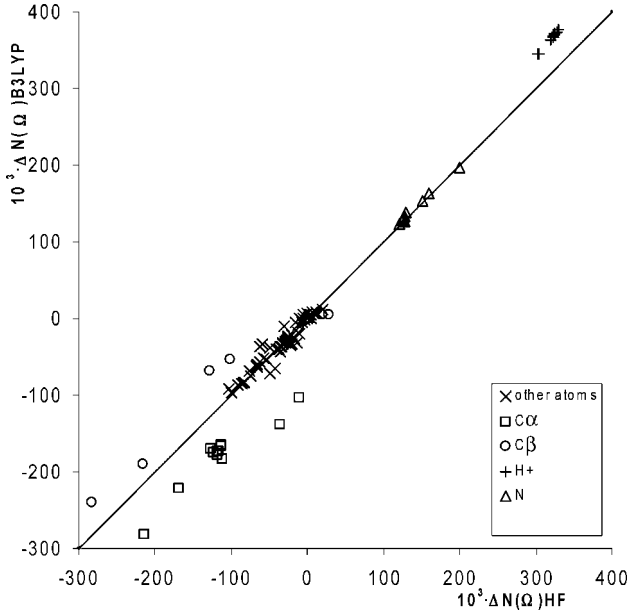

Figure 1. Variations experienced by the atomic populations, $\Delta N(\Omega)$, of **1**−**12** upon N-protonation as computed from HF and B3LYP electron densities. All values in au multiplied to 10^3. The line shown in plot corresponds to the ideal $\Delta N^{HF}(\Omega) = \Delta N^{B3LYP}(\Omega)$ equivalence.

and Jensen[31] until the molecular virial ratio, γ, obtained differs from its ideal value by less than 3×10^{-6}. This procedure has proved to solve[32] shortcomings previously reported for QTAIM atomic energies.[33] Nevertheless, as the atomic energies are obtained by correcting atomic electron kinetic energies, $K(\Omega)$, with γ, and part of the electron kinetic energy is considered in DFT within the exchange-correlation term, we will only made use of $E(\Omega)$ values obtained with HF electron densities. In contrast, for the sake of simplicity, we will only refer to B3LYP $N(\Omega)$ electron populations. In this case, both computational levels give rise to different absolute $N(\Omega)$ values, but the relative values obtained for the protonation process, $\Delta N(\Omega)$, are significantly similar and correlated (Figure 1) if we exclude some exceptions like the decrease of electron population at the C of the cyano group, which is always more depleted according to the B3LYP level (around 0.055 au more, but in delocalized systems **11**−**15** where the difference exceeds 0.09 au). Significant differences between $\Delta N^{HF}(\Omega)$ and $\Delta N^{B3LYP}(\Omega)$ values are also observed for the C in α to the cyano group in delocalized systems. They range is from 0.049 au in **13** to 0.061 au in **11**.

The electron densities obtained were analyzed with the QTAIM by means of the program *AIMPAC*.[34,35] The accuracy of the integrated properties was tested using the differences between molecular properties and those obtained by summation of the properties of the fragments [$N - \Sigma N(\Omega)$ or $E - \Sigma E(\Omega)$] (Table 1). These differences are always smaller (in absolute value) than 2×10^{-3} au and 1.2 kJ/mol respectively, which are found to be accurate enough comparing with other works carried out at similar theoretical levels. In the same vein, the integrated values of the laplacian of the electron density in all of the atomic fragments, $L(\Omega)$, are always smaller (in absolute value) than 10^{-3} au.

Proton affinities at the N atom (Table 1) were calculated taking into account the thermal and zero point vibrational corrections (unscaled) obtained for protonated and neutral species. The correction term for transforming reaction internal energies into reaction enthalpies was considered as well.

Results and Discussion

Atomic and bond properties of neutral nitriles, as well as the $\nabla^2\rho(\mathbf{r})$ topology, have been described thoroughly in a previous HF study by Aray et al.[36] As our results for neutral molecules are in perfect agreement with theirs, we focus our discussion on the effects of protonation.

Proton Affinities. There is a reasonable agreement between computed and experimental[37] proton affinities (PAs), which are slightly improved at the B3LYP/6-31++G(d,p) level with regard to the HF/6-31++G(d,p) one (Table 1) and previous HF values obtained with smaller basis sets.[38] The only exception for this general trend is benzonitrile, **13**, where the HF/6-31++G(d,p) PA is closer to the experimental one. This molecule displays the largest discrepancy between B3LYP and experimental PA (18 kJ mol^{-1}), whereas most of them are below 10 kJ mol^{-1}.

The largest PAs correspond to delocalized systems **12**−**15**. In fact, according to Table 1, PAs of nitriles increase with molecular size and π-delocalization. Also, cyanoalkanes **2**−**9** display a good linear correlation ($r^2 = 0.98$) between PAs and N(H^+) (Figure 2). PAs of delocalized **11**−**15** apart less than 7 kJ mol^{-1} from this fitting line, whereas **1** and **10** are clear outliers.

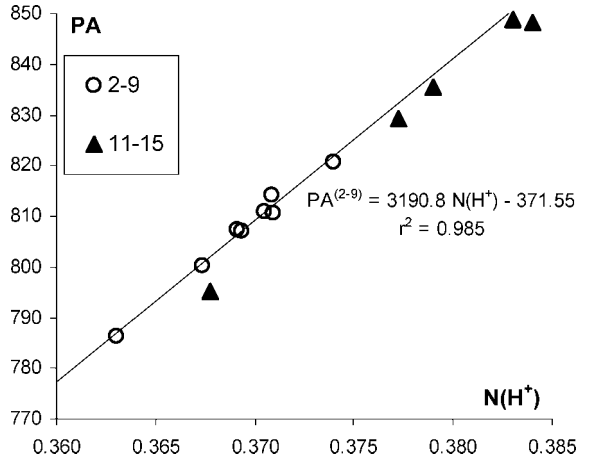

Figure 2. Plot of B3LYP/6-31++G(d,p) PAs (in kJ mol^{-1}) vs N(H^+) (in au) for **2**−**9** and **11**−**15**. The fitting line corresponds to alkyl **2**−**9**. Compounds **1** and **10** are clearly outside of this linear fitting and are not shown in the figure.

The PA values shown in Table 1 could be taken as an indication that electron delocalization raises the PA. Nevertheless, we should also notice that the size of the substituents, and more concretely the number of hydrogens in the molecule, increase PA values. Thus, when we compare PAs obtained for saturated and unsaturated substituents with similar size or similar number of hydrogens (e.g., **3** and **11**) we realize the PA for a nitrile bearing an unsaturared substituent is lower than that for the corresponding compound with a saturated group.

Protonation Effects on Atomic Electron Populations. As a general trend, we observe (Figure 3) that the proton keeps a very positive charge when attached to the cyanocompound (always larger than +0.62 au), which is more in line with a $H^+-N\equiv C-R$ Lewis structure than with the $H-N^+\equiv C-R$ and $H-N=C^+-R$ ones. This charge is more positive than that computed at the same level for the N-protonated forms of pyrimidinic bases (+0.48 to +0.51 au).[7] They are also larger than those computed at the MP2/6-311++G(d,p) level for protonated methylamine (+0.477 au) and protonated methylenimine (+0.511 au).[9] As the computational level does not affect very much QTAIM charges, we can say that the positive charge at the proton grows with the s character of N hybridization. This trend was not found for O-protonations, where the atomic charge of the proton remains around +0.66 au independently on the O hybridization as shown with MP2/6-31++G(d,p) studies on linear alkyl ethers[13] and ketones[39] and B3LYP/6-31++G(d,p) studies on cyclic ethers[14] and pyrimidinic bases.[7]

The electron density of the molecule evolves upon protonation following the mechanism previously reported for other O-protonations[7−9,21] and N-protonations.[7,8,20,21] Thus, for **1** the electron density gained by the proton is provided by the N atom, which loses 0.335 au of σ electron density and 0.010 au of π electron density. Nevertheless, the electron population of the N atom is not reduced in the protonated form, but enlarged. This is due to the deformation of the electron density in the whole molecule produced by the proton, which gives rise to electron density transferences between neighboring atoms.[8] Thus, N receives from C 0.360 and 0.112 au of σ and π density respectively in **1**. At the same time, the H atom transfers 0.171 and 0.019 of σ and π electron density to the C. It can be observed that the proton enlarges more the polarization of the π density in N≡C than in the σ one. The reason may be that the σ electron pair is already much more polarized than the π ones in the neutral molecule (1.575 au of the σ pair belongs to the N basin, whereas

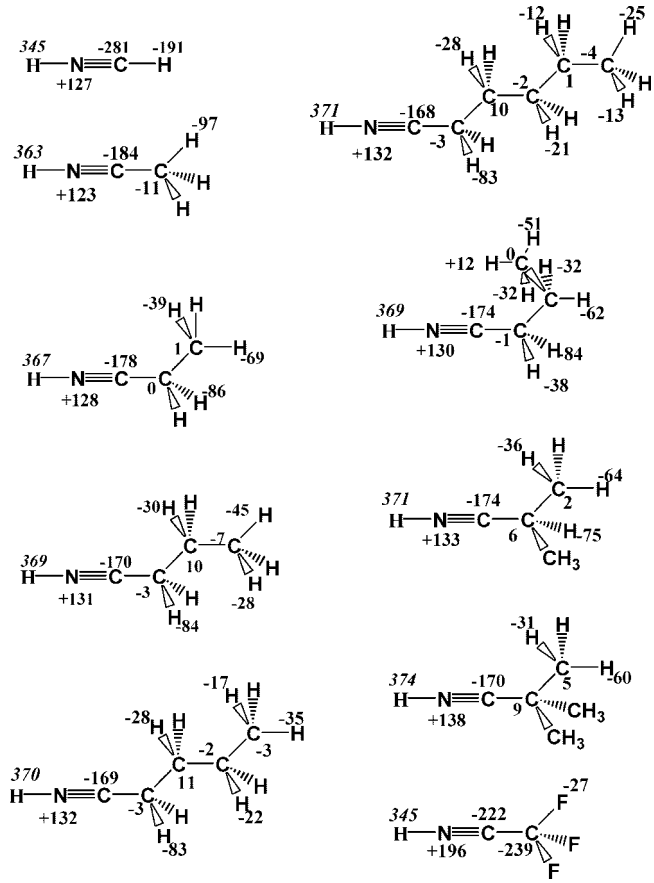

Figure 3. Variations of atomic electron population, $\Delta N(\Omega)$, experienced upon protonation by **1**−**10** (in au multiplied by 10^3) and electron population gained by the proton (in italics). $\Delta N(\Omega)$ is only shown for one of those atoms related by symmetry.

TABLE 2: Variations of Atomic π-Electron Population (in au Multiplied by 10^3) Experienced by 11−15 upon Protonation; ΔN(R) Indicates the Summation of π and σ Atomic Electron Populations Experienced by the Whole R Group.

	ΔN^{π}(N)	$\Delta N^{\pi}(C_{CN})$	$\Delta N^{\pi}(C_{\alpha})$	$\Delta N^{\pi}(C_R)$	ΔN(R)
11	233	−75	32	−143	−139
12	265	−30	50	−216	−194
13	250	−47	53	−189	−201
14	264	−23	53	−225	−248
15	263	−28	54	−220	−233

1.331 au of each of the π pairs are within that basin, all data taken from molecule **1**).

When the H of HCN is replaced by an alkyl group, the electron population lost by the C atom is significantly reduced. This is due to the σ electron density provided by the neighboring alkyl group, R, which increases with the size of the group, though approaching a convergence limit. Thus, the electron density provided by R represents approximately $^2/_3$ parts of the total electron transference for a long chain cyanoalkane, like **6**. Most of this electron population supplied by the alkyl group comes from the depletion of hydrogen electron populations. In fact, the electron populations of the carbons in the alkyl group (**2**−**10**) present little variations that are sometimes positive (Figure 3). $\Delta N(\Omega)$ variations experienced by each of the hydrogen atoms can be rationalized using the scheme presented in previous papers to explain the protonation trends of uracil[8] and cytosine.[21] Thus, (i) the closer the distance to the proton, the easier the electron density donation; and (ii) the donation

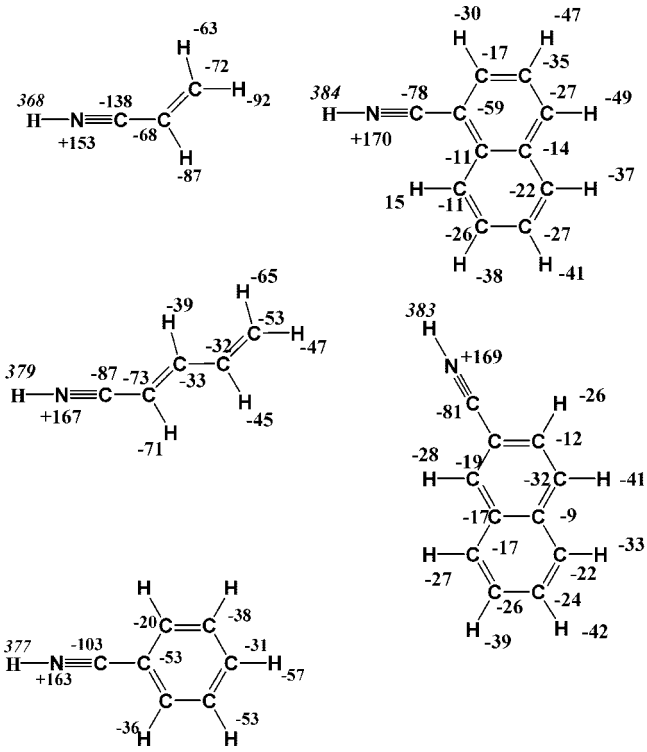

Figure 4. Variations of atomic electron population, $\Delta N(\Omega)$, experienced upon protonation by **11**−**15** (in au multiplied by 10^3) and electron population gained by the proton (in italics). $\Delta N(\Omega)$ is only shown for one of those atoms related by symmetry.

of electron population between bonded atoms follows the direction of the bond. The orientation of the bond with regard to the proton makes the electron transference easier (when the electron density approaches the proton) or more difficult (when the electron density moves away the proton). Thus, for instance, the hydrogens bonded to C_3 in butanenitrile **4** lose less electron population (−0.030 au) than the hydrogen in antiperiplanar arrangement bonded to C_4 (−0.045 au) (Figure 3).

When the alkyl chain experiences an internal rotation, as from **4** to **7**, the only $\Delta N(\Omega)$ values significantly affected are those of the group rotated, where the electron transfers among the diverse atoms are reorganized taking into account the new orientation and distances to the proton, as can be seen in Figure 3. We have also considered an eclipsed conformation of the terminal methyl for this compound, where the two out of plane hydrogens are in favorable orientations to transfer electron density to C_4 and the in plane hydrogen orientates its C−H bond moves electron density away the proton. The result is the former experiences depletions of −0.040 au in the protonated form, whereas the later only reduces its population in −0.021 au.

The presence of branched substituents, like Pr^i (in **8**) or Bu^t (in **9**) has qualitatively the same effect as the enlargement of the alkyl chain. Nevertheless branched substituents are quantitatively more efficient to increase the electron donation, as they arrange more hydrogens close to the proton, which act as electron density sources. Thus, it can be observed that Pr^i experiences larger transferences than Pr^n, Bu^n, and even Pe^n (Figure 3). This is also true for Bu^t, but this substituent does not suppose any increase of electron transference with regard to Pr^i.

When the hydrogens of **2** are replaced by much more electronegative atoms, like in **10**, the electron population transferred to the proton is reduced. In this case, the carbon of the CF_3 group is the largest donor. It is also significant that

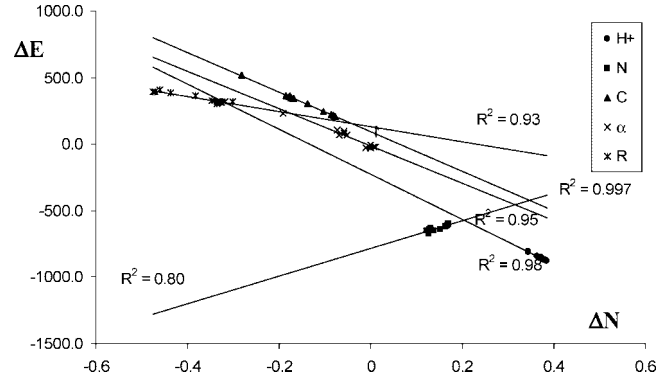

Figure 5. Relationship between the variations in atomic energies and populations as a result of protonation.

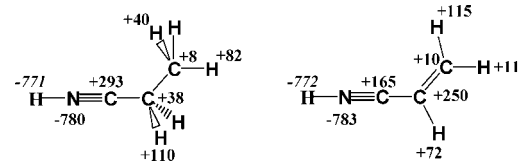

Figure 6. Variation of atomic energy, $\Delta E(\Omega)$, (in kJ mol^{-1}) experienced upon protonation by **3** and **11** and electronic energy gained by the proton (in italics). $\Delta E(\Omega)$ is only shown for one of those atoms related by symmetry.

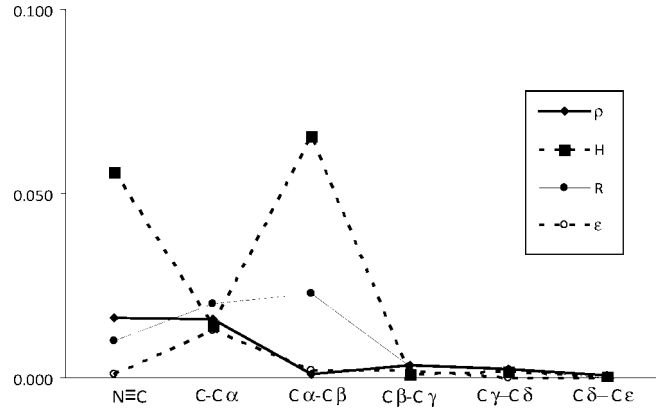

Figure 7. Plot of variations experienced (all values are in au but R is in Å) upon protonation by the bond properties in molecule 6. Values refer to differences between protonated and neutral molecules in absolute values.

electron density gained by the nitrogen achieves its maximum in the series (Figure 3).

The protonation of nitriles that contain π-conjugated substituents shows a significant contrast with that of cyanoalkanes (Table 2). Thus, the carbon atoms of the substituent experience an important reduction of π-electron density upon protonation, whereas the σ-electron density remains practically unchanged as in cyanoalkanes. This reduction of $N^{\pi}(C)$ is combined with smaller donations from hydrogen atoms. Nevertheless, π-electron transferences from the substituent in the molecules here studied (**11**−**15**) are so large that the total transferences to the protonated nitrile exceed always those observed for large cyanoalkanes (showing larger electron density increases at N and the proton). It is also significant that the electron density lost by the carbon of the nitrile group upon protonation is much smaller in molecules with conjugated substituents than in cyanoalkanes. We also observe that the amount of π-electron density donated increases with the size of the substituent.

The protonations of α and β isomers of cyanonaphtalene involve very similar electron transfers, moving 0.476 and 0.471

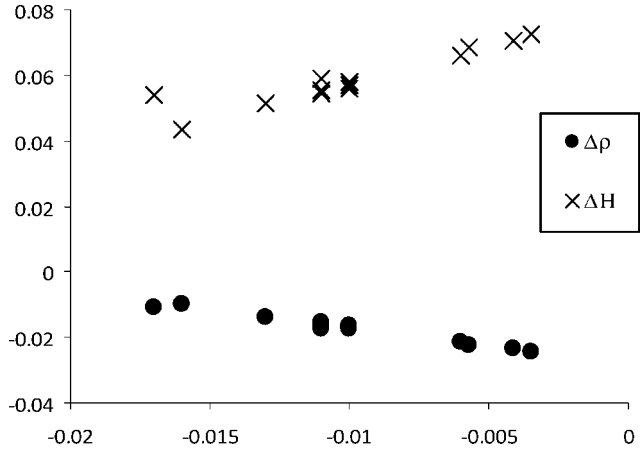

Figure 8. Plot of variation of $\rho(\mathbf{r}_c)$ and $H(\mathbf{r}_c)$ vs the variation of the distance of the C−N bond. Values refer to differences between protonated and neutral molecules. All values are in au but ΔR is in Å.

au from the bicyclic systems to the H^+−NC region, respectively. The most significant $\Delta N(\Omega)$ difference between both systems corresponds to the α hydrogen of the unsubstituted cycle that is in cis arrangement to the cyano group, $H^{\alpha c}$. We can observe (Figure 4) that $\Delta N(H^{\alpha c})$ is positive (+0.015 au) for α-cyanonapthalene and negative (−0.027 au) for β-cyanonaphtalene, whereas the remainig ΔN(H) and ΔN(C) couples of values do not differ by more than 0.008 au (excluding the C−H group next to the nitrile group that is α in the former and β in the latter). $\Delta N(H^{\alpha c})$ in α-cyanonapthalene is the only positive value observed in the R group of both molecules. It can be explained because of the proximity between $H^{\alpha c}$ and the proton attached to the cyano group. This proximity provides an easy way for approaching electron density in the unsubstituted ring to the proton. The different position and orientation of the CN group in β-cyanonaphtalene prevents this mechanism and $H^{\alpha c}$ plays its usual role in protonations as electron source.

Protonation Effects on Atomic Energies. Figure 5 shows the relationships between the variations in atomic energies and populations as a result of protonation. Good correlations are found when **10** is excluded. For C atoms, R groups, and protons, atomic energies become more negative as populations increase, whereas for N atoms the opposite effect is found. Also, N atoms exhibit the worst correlation factor ($R^2 = 0.80$). As it could be inferred from Figure 5, α atoms show the smallest variations in both energies and populations because they are farther from a proton than atoms in the CN group. For R groups, differences for several atoms are summed up, but if separated atoms were considered the same effect could be found, that is as the distance from the proton increases the differences decrease. It is also noticeable that these atoms are those where variations of $N(\Omega)$ provide the smallest effect on $E(\Omega)$. The only atom stabilized by protonation is the N atom of the CN group, which is the only one gaining electron density upon protonation in all of the molecules. Thus, the positive values of PAs came from the stabilization gained by N and proton, which exceeds the destabilization experienced by the remaining atoms.

Comparing molecules with saturated and unsaturated substituents of similar size (**3** and **11**), we notice (Figure 6) that the smallest reduction of electron density in the carbon of the CN group when R is unsaturated gives rise to a smaller atomic destabilization in the protonated compound. In contrast, R unsaturated groups result much more destabilized upon protonation (563 kJ mol^{-1} in **11** vs 428 kJ mol^{-1} in **3**, or 525 kJ mol^{-1} in **13** vs 440 kJ mol^{-1} in **6**). Overall, the summation of atomic destabilization in **11**−**15** exceeds that of comparable saturated compounds.

Protonation Effects on Bond Properties. The effects of N-protonation on the bond properties could be exemplified by cyanohexane (**6**) (Figure 7). In this molecule, it can be observed that, as a general rule, the effects on the bond properties (R, $\rho(\mathbf{r}_c)$, $H(\mathbf{r}_c)$, and ε) decrease as the distance to the proton increases. Nevertheless, significant fluctuations are found as we move further in the alkyl chain: so, $H(\mathbf{r}_c)$ shows higher differences for the Cα−Cβ bond than for the C−Cα one. Figures 8 and 9 show variations of $\rho(\mathbf{r}_c)$, and $H(\mathbf{r}_c)$ regarding to variations in C≡N and C−C bond lengths, respectively. Both figures exhibit almost linear relationships. $\Delta\varepsilon$ values are not shown as they are always very small.

For all C≡N bonds, the bond shortens upon protonation ($\Delta R < 0$), whereas $\rho(\mathbf{r}_c)$ decreases ($\Delta\rho(\mathbf{r}_c) < 0$) and $H(\mathbf{r}_c)$ becomes less negative ($\Delta H(\mathbf{r}_c) > 0$). The shortening of the C≡N bond is apparently contradictory with changes found for $\rho(\mathbf{r}_c)$ and $H(\mathbf{r}_c)$, which could be associated to the decrease of charge

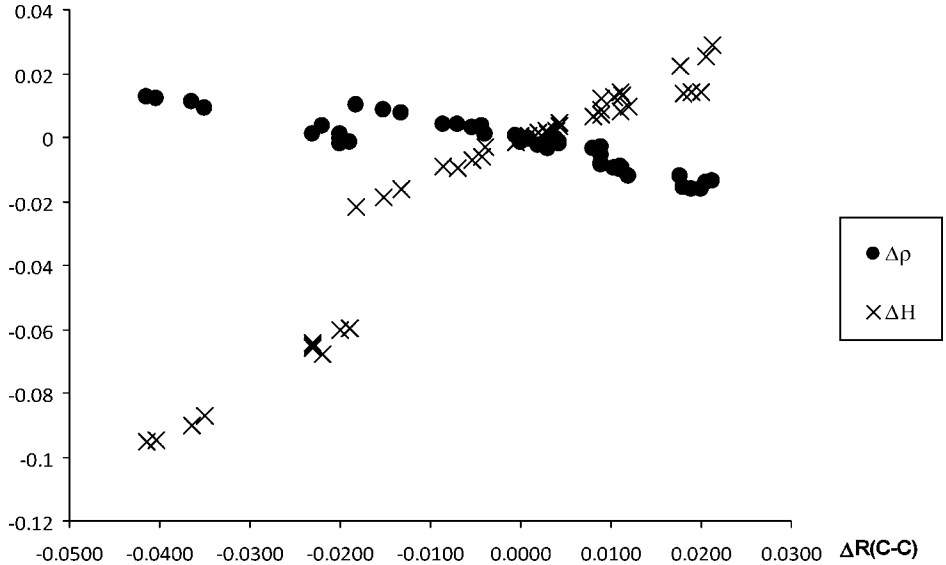

Figure 9. Plot of variation of $\rho(\mathbf{r}_c)$ and $H(\mathbf{r}_c)$ vs the variation of the distance of the C−C bonds. Values refer to differences between protonated and neutral molecules. All values are in au but ΔR is in Å.

density in the bond critical point and so to the weakening of the bond. However, it should be taken into account that the properties in the bond critical point only reflect what happens to σ density as the π density is out of the plane of the bond. Then, the shortening of the bond length and the changes in bond properties upon protonation are compatible with the increase of the π density and the decrease of the σ density in the C≡N bond, which confirms the important π character of the C≡N bond in protonated compounds and so the predominance of the resonance form containing a triple bond ($H^+-N\equiv C-R$).

From Figure 9 it could be inferred that when the bond length remains constant all of the properties of the BCP remain also unchanged. This happens for C−C bonds placed further away within the R group. The most negative values of ΔR correspond to the most negative ones of $\Delta H(\mathbf{r}_c)$ and to the most positive ones of $\Delta\rho(\mathbf{r}_c)$. So, when the bond shortens, bond properties reflect a strengthening of the bond, whereas the opposite happens when the bond lengthens.

Conclusions

After the protonation of cyanocompounds, the proton keeps a very positive charge, which is more in line with a $H^+-N\equiv C-R$ Lewis structure than with the $H-N^+\equiv C-R$ and $H-N=C^+-R$ ones. This is also confirmed by the increase of the π density and the decrease of the σ density in the C≡N bond obtained from results of its bond properties.

The electron density of HCN evolves upon protonation following the mechanism previously reported for other O-protonations[7−9,21] and N-protonations[7,8,20,21] due to the deformation of the electron density in the whole molecule produced by the proton, which gives rise to electron density transferences between neighboring atoms. When the H of HCN is replaced by an alkyl group the electron population lost by the C atom is significantly reduced, due to the σ-electron density provided by the neighboring alkyl group, R. When the alkyl chain experiences an internal rotation, the only $\Delta N(\Omega)$ values significantly affected are those of the group rotated. For nitriles with π-conjugated substituents, an important reduction of π-electron density appears upon protonation, whereas the σ-electron density remains practically unchanged as in cyanoalkanes.

Also, we have found a reasonable agreement between experimental and calculated PA values as well as good correlations between variations in atomic energies and populations as a result of protonation.

Acknowledgment. We are indebted to "Centro de Supercomputación de Galicia" (CESGA) for access to their computational facilities and to "Xunta de Galicia" and Spanish MEC for financial support through, respectively, projects C217122P-64100 and CTQ2006-15500/BQU.

References and Notes

(1) Carey, F. A.; Sundberg, R. J. *Advanced Organic Chemistry*; Kluwer Academic: New York, 2001.
(2) Wheland, G. W. *Resonance in Organic Chemistry*; Wiley: New York, 1955.
(3) Bader, R. F. W. *Atoms in Molecules: A Quantum Theory*; Oxford University Press: New York, 1990.
(4) Bader, R. F. W. *Chem. Rev.* **1991**, *91*, 893.
(5) Wiberg, K. B.; Laidig, K. E. *J. Am. Chem. Soc.* **1987**, *109*, 5935.
(6) Wiberg, K. B.; Breneman, C. M. *J. Am. Chem. Soc.* **1992**, *114*, 831.
(7) González Moa, M. J.; Mosquera, R. A. *J. Phys. Chem. A* **2003**, *107*, 5361.
(8) González Moa, M. J.; Mosquera, R. A. *J. Phys. Chem. A* **2005**, *109*, 3682.
(9) Mandado, M.; Van Alsenoy, C.; Mosquera, R. A. *J. Phys. Chem. A* **2004**, *108*, 7050.
(10) Mandado, M.; Van Alsenoy, C.; Mosquera, R. A. *Chem. Phys. Lett.* **2005**, *405*, 10.
(11) Glaser, R.; Choy, G. S. K. *J. Am. Chem. Soc.* **1993**, *115*, 2340.
(12) Vila, A.; Mosquera, R. A. *J. Phys. Chem. A* **2000**, *104*, 12006.
(13) Vila, A.; Mosquera, R. A. *Chem. Phys. Lett.* **2000**, *332*, 474.
(14) Vila, A.; Mosquera, R. A. *Tetrahedron* **2001**, *57*, 9415.
(15) Perrin, C. *J. Am. Chem. Soc.* **1991**, *113*, 2865.
(16) Laidig, K. E. *J. Am. Chem. Soc.* **1992**, *114*, 7912.
(17) Gatti, C.; Fantucci, P. *J. Phys. Chem.* **1993**, *97*, 11677.
(18) Hirshfeld, F. L. *Theor. Chim. Acta* **1977**, *44*, 129.
(19) De Proft, F.; Van Alsenoy, C.; Peeters, A.; Langenaker, W.; Geerlings, P. *J. Comput. Chem.* **2002**, *23*, 1198.
(20) Otero, N.; González.Moa, M. J.; Mandado, M.; Mosquera, R. A. *Chem. Phys. Lett.* **2006**, *428*, 249.
(21) González Moa, M. J.; Mandado, M.; Mosquera, R. A. *Chem. Phys. Lett.* **2006**, *428*, 255.
(22) Stutchbury, N. C. J.; Cooper, D. L. *J. Chem. Phys.* **1983**, *79*, 4967.
(23) Alcoba, D. R.; Lain, L.; Torre, A.; Bochicchio, R. C. *Chem. Phys. Lett.* **2005**, *407*, 379.
(24) Cioslowski, J.; Mixon, S. T. *Can. J. Chem.* **1992**, *70*, 443.
(25) Bader, R. F. W. *J. Phys. Chem. A* **1998**, *102*, 7314.
(26) Haaland, A.; Shorokhov, D. J.; Tverdova, N. V. *Chem.—Eur. J.* **2004**, *10*, 4416.
(27) Poater, J.; Sola, M̀.; Bickelhaupt, F. M. *Chem.—Eur. J.* **2006**, *12*, 2889.
(28) Bader, R. F. W. *Chem.—Eur. J.* **2006**, *12*, 2896.
(29) Poater, J.; Sola, M̀.; Bickelhaupt, F. M. *Chem.—Eur. J.* **2006**, *12*, 2902.
(30) *GAMESS*: Schmidt, M. W.; Baldridge, K. K.; Boatz, J. A.; Elbert, S. T.; Gordon, M. S.; Jensen, J. H.; Koseki, S.; Matsunaga, N.; Nguyen, K. A.; Su, S. J.; Windus, T. L.; Dupuis, M.; Montgomery, J. A. *J. Comput. Chem.* **1993**, *14*, 1347–1363.
(31) Lehd, M.; Jensen, F. *J. Comput. Chem.* **1991**, *12*, 1089.
(32) Cortes-Guzmán, F.; Bader, R. F. W. *Chem. Phys. Lett.* **2003**, *379*, 183.
(33) Mandado, M.; Vila, A.; Graña, A. M.; Mosquera, R. A.; Cioslowski, J. *Chem. Phys. Lett.* **2003**, *371*, 739.
(34) Bader, R. F. W. et al. *AIMPAC: A Suite of Programs for the AIM Theory*; McMaster University: Hamilton, Ontario, Canada, L8S 4M1. Contact bader@mcmail.cis.mcmaster.ca.
(35) Biegler-Konig, F. W.; Bader, R. F. W.; Nguyen-Dang, T. T. *J. Comput. Chem.* **1982**, *3*, 371.
(36) Aray, Y.; Murgich, J.; Luna, M. A. *J. Am. Chem. Soc.* **1991**, *113*, 7135.
(37) Hunter, E. P.; Lias, S. G. *J. Phys. Chem. Ref. Data* **1998**, *27*, 413.
(38) Mariott, S.; Topsom, R. D.; Lebrilla, C. B.; Koppel, I.; Mishima, M.; Taft, R. W. *J. Mol. Struct.* **1986**, *137*, 133.
(39) Graña, A. M.; Mosquera, R. A. *Chem. Phys.* **1999**, *243*, 17.

JP811023X